Talanta 82 (2010) 1448–1454

Contents lists available at ScienceDirect

Talanta

journal homepage: www.elsevier.com/locate/talanta

Characterization of home-made silver sulphide based iodide selective electrode

A. Rajbhandari (Nyachhyon)*, A.P. Yadav, K. Manandhar, R.R. Pradhananga

Central Department of Chemistry, Tribhuvan University, Kirtipur, Kathmandu, Nepal

ARTICLE INFO

Article history:
Received 30 May 2010
Received in revised form 4 July 2010
Accepted 9 July 2010
Available online 16 July 2010

Keywords:
Iodide selective electrode (ISE)
Silver sulphide
Silver iodide
Nernstian response
Mott–Schottky analysis

ABSTRACT

Polycrystalline silver sulphide/silver iodide ion selective electrodes (ISEs) with four different compositions, 9:1, 2:1, 1:1, 1:9 Ag_2S–AgI mole ratios, have been fabricated in the laboratory and characterized by X-ray diffractometry (XRD), scanning electron microscopy (SEM), and electrochemical impedance spectroscopy (EIS). X-ray diffraction studies show the presence of Ag_3SI, Ag_2S and AgI crystalline phases in the electrode material. The electrode surfaces have been found to become smoother and lustrous with increasing percentage of silver sulphide in silver iodide. ISE 1:1, ISE 2:1 and ISE 9:1 all responded in Nernstian manner with slopes of about 60 mV/decade change in iodide ion concentration in the linear range of 1×10^{-1} to 1×10^{-6} M while ISE 1:9 showed sub-Nernstian behavior with slope of about 45 mV up to the concentration 1×10^{-5} M. Two capacitive loops, one corresponding to the charge transfer process at metal electrode and the back contact and a second loop corresponding to the charge transfer process at membrane–electrolyte interface have been observed at high and low frequency ranges, respectively. Mott–Schottky analysis shows that the materials are n-type semiconductors with donor defect concentrations in the range of 5.1×10^{14} to $2.4 \times 10^{19}/cm^3$.

1. Introduction

Ion selective electrodes (ISE) are powerful analytical tools for the quantitative determination of various ions in solution. These electrodes have been used in varieties of fields like pharmaceutical, environmental, medical, industrial fields as they provide rapid, accurate and low cost methods of analysis [1–5]. A number of ISEs are commercially available which are selective for various cations and anions [6–14]. Silver sulphide based ISEs are well known for being well behaved electrodes in terms of their sensitivity and selectivity and have been in operation for long [15,16]. The sensitivity and selectivity of such electrodes towards target ions depend on the membrane composition, method of preparation and the surface morphology. Silver sulphide/silver iodide all solid state ion selective electrodes prepared by Ruziicka and Lamm [17] were found to have a life span of only about 35 days. Limited information regarding surface morphology, phase composition and electron transfer processes at electrode–electrolyte interface on those electrodes is available [18].

Electrochemical impedance spectroscopy (EIS) is a sensitive and non-destructive technique to obtain information on the electron-transfer resistance and capacitive behavior of electrode–electrolyte interface. Only a very few EIS studies [19–22] have been reported on silver sulphide based ISEs. Semiconductor behavior and the donor/acceptor density of silver sulphide based ISEs were studied by Bard and Faulker [23].

In the present study, iodide ion selective electrodes of four different compositions; 9:1, 2:1, 1:1, 1:9 mole ratio of Ag_2S–AgI were fabricated and characterized by XRD, SEM and electrochemical techniques. Electrochemical impedance spectroscopy (EIS) technique was also used to investigate their electrical properties. Capacitance measurements were done to evaluate the donor defect concentration of the materials by Mott–Schottky analysis. Finally, the effects of storage of electrode in iodide solution on the surface of membrane were also investigated.

2. Experimental

2.1. Chemicals and solutions

All the Chemicals ($AgNO_3$, KI, KBr, KCl, Na_2S, and KNO_3) used were of analytical grade and all the solutions were prepared in distilled water. Direct potentiometry was carried out by successive addition of iodide solution in 0.1 M KNO_3, which was used as the background electrolyte. A stock solution of 0.1 M $AgNO_3$ (S.D. Fine) and 0.1 M KI (Merck) were prepared. The stock solution of 0.1 M Na_2S (LR grade) solution was prepared and standardized with potassium iodate solution by standard method [24].

---

* Corresponding author. Tel.: +977 1 4332034.
E-mail address: armila3@yahoo.com (A. Rajbhandari (Nyachhyon)).

0039-9140/$ – see front matter © 2010 Elsevier B.V. All rights reserved.
doi:10.1016/j.talanta.2010.07.016

Table 1
Composition of home-made electrodes.

Mole ratio of Ag_2S:AgI	Mole% of Ag_2S	Mole% of AgI
9:1	90	10
2:1	67	33
1:1	50	50
1:9	10	90

2.2. Apparatus

XRD analysis was performed to investigate the crystal phase of the electrode materials using an X'Pert MPD-OEC, Phillips X-ray diffractometer. The measurements were performed using Cu kα radiation at 40 kV and 40 mA. Scanning electron microscopy (SEM) characterization was performed with a KEYENCE REAL 3D System, VE-series, Japan at 5 kV accelerating voltage. The electrochemical impedance measurements were performed using a Solartron 1280 Schlumberger frequency response analyzer. The impedance spectra were recorded in the frequency range between 10 kHz and 20 kHz at 10 mV perturbing signal and Z-view software (version 2.6 b) was used for evaluating the impedance spectra.

2.3. Preparation of membrane material and electrode

In the present study, iodide selective electrodes with four different compositions were prepared by co-precipitation of Ag_2S and AgI in different mole ratios. Desired mole ratio of Ag_2S:AgI membrane was obtained by taking appropriate moles of aqueous solution of Na_2S and KI in which slight excess of aqueous solution of $AgNO_3$ was added. The reaction is given in Eq. (1).

$$KI + Na_2S + 3\,AgNO_3 \rightarrow Ag_2S + AgI + 2NaNO_3 + KNO_3 \qquad (1)$$

Table 1 shows the compositions of four different samples of Ag_2S:AgI.

The co-precipitate of Ag_2S–AgI was filtered and washed five times with distilled water. The final wash was done with acetone. The material thus obtained was dried at 110 °C for 6 h. The dried material was ground to fine powder in an agate mortar. About 1.5 g of fine powder of Ag_2S–AgI was taken in a KBr pellet making die. The powder was pressed under 10 tonnes/cm^2 pressure for 15 min to make a pellet. The pellet was removed carefully from the die and was dried at 200 °C for an hour. The prepared pellet was then mounted in a polypropylene tube with the help of Araldite (Ciba–Geigy) and back contact was made with silver epoxy conducting paint with silver disk in which a copper wire was soldiered. The electrode was polished successively with 1000–2000 grit sized silicon carbide paper and finally carefully sonicated in distilled water.

All the measurements were performed using Ag/AgCl (sat.) electrode as reference electrode.

3. Results and discussion

3.1. Characterization of membrane material

The co-precipitate of Ag_2S–AgI was characterized by XRD to know the crystalline phase present in the electrode material. Fig. 1 shows the diffraction pattern of all the samples. The diffraction peaks matched with that of Ag_2S, Ag_3SI and AgI compounds. The assignments based on the JCPDS data are given for the respective main diffraction peaks in the figure. In sample 9:1, 2:1 and 1:1 the peaks at 25.8°, 31.8°, and 36.8° were assigned for Ag_3SI while the peaks at 34.7°, 36.8°, 37.9° were assigned for Ag_2S and 23.8°, 39.3°, and 45.4° peaks were assigned to that of AgI. The presence of Ag_3SI along with Ag_2S and AgI shows that the materials are in mixed phase state.

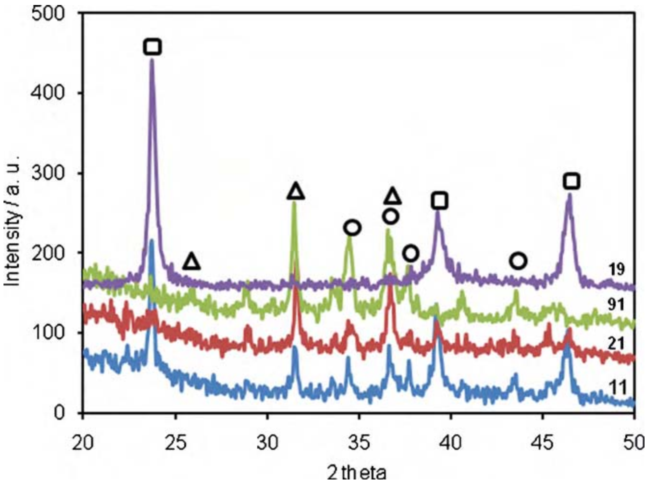

Fig. 1. XRD Pattern of laboratory prepared electrodes of various composition of Ag_2S–AgI. The peaks are indicated by symbols: (○) for Ag_2S, (△) for Ag_3SI, and (□) for AgI.

In diffraction peaks of sample no. 4 with 90% AgI, some minor peaks of Ag_2S appeared along with three intense peaks of AgI.

3.2. Characterization of electrode

3.2.1. Scanning electron micrograph studies

The surface morphology of an ISE is one of the important factors that control the quality of electrode. In the present study, variation of the surface morphology with the amount of Ag_2S and AgI in the co-precipitates was analyzed by taking SEM photographs of polished surface. Fig. 2a–d shows the SEM photographs of all the four samples taken at 5 kV of accelerating voltage. It is obvious that the surface texture changes with the composition of the co-precipitate. In first sample, the surface was smooth and fine with small white patches while in 2nd and 3rd samples, the size of white patches increased. The 4th sample was rough having more bright parts. So, it seems reasonably to conclude that the sample having high percentage of Ag_2S causes lustrous and smooth surface morphology.

3.2.2. Potentiometric behavior of the electrodes

The potentiometric responses of ISE 9:1, ISE 2:1, ISE 1:1 and ISE 1:9 to iodide ions are shown in Fig. 3. Appropriate spikes of iodide were introduced into the cell and corresponding potentials were recorded. To maintain a constant ionic strength, 0.1 M KNO_3 solution was used in all measurements. All measurements were carried out at constant stirring condition. The plot of potential against negative logarithm of iodide concentration is shown in Fig. 3.

Fig. 3 shows that ISE 9:1, ISE 2:1 and ISE 1:1 all give a linear response with respect to $[I^-]$ in the region 1×10^{-1} to 1×10^{-6} M with slopes ranging from 54 to 60 mV. In the lower concentration range the curves however start to deviate from linearity. The slopes and linear region of all the electrodes are tabulated in Table 2. The electrode with 10 percentage Ag_2S and 90 percentage AgI deviated from linearity much earlier and showed the sub-Nernstian behavior from the beginning with the slope of about 45 mV/decade $[I^-]$ up to 1×10^{-5} M.

3.2.3. The response time of the electrode

The response time of the electrodes was measured with steps of 10-fold increase of the concentration of iodide ion. It was observed that the response was fast, and the system attained equilibrium

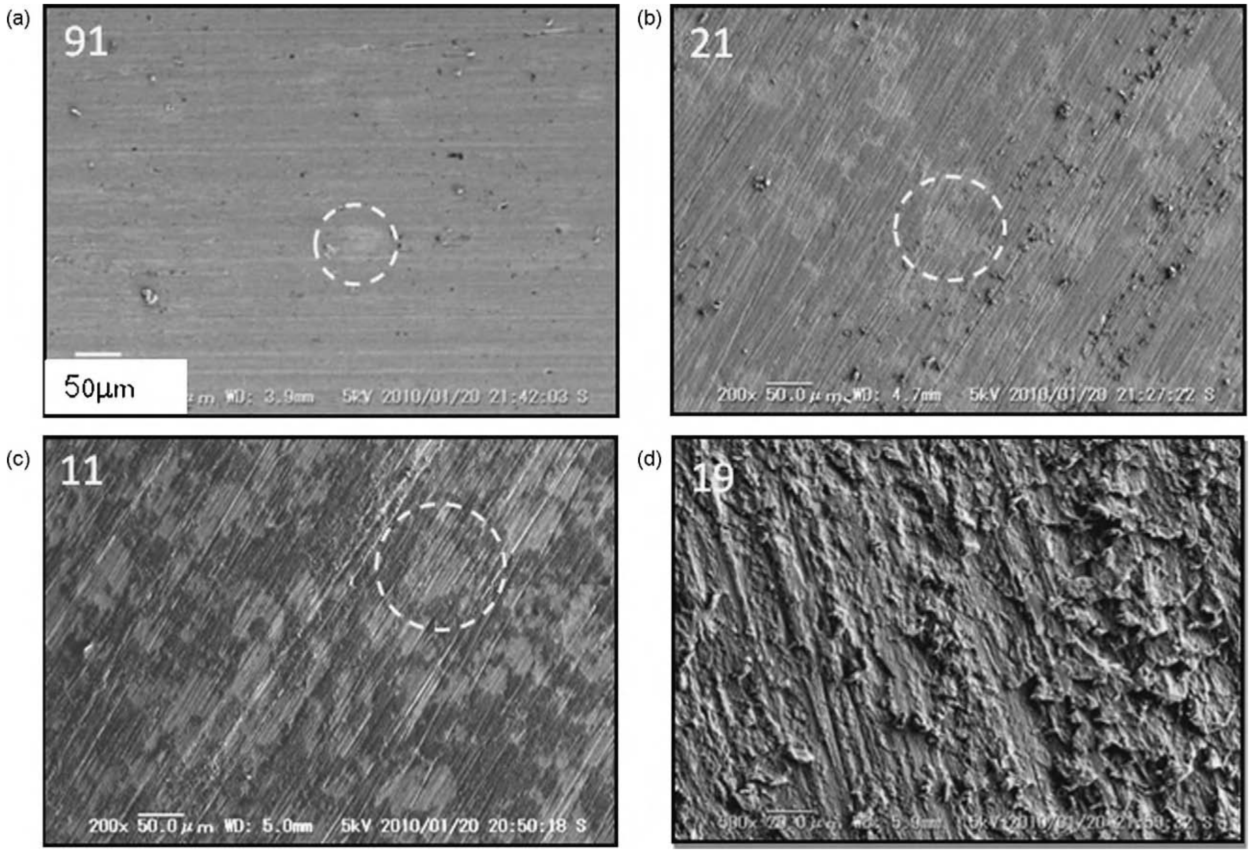

Fig. 2. (a–d) SEM pictures of as polished surface of Ag_2S/AgI electrodes.

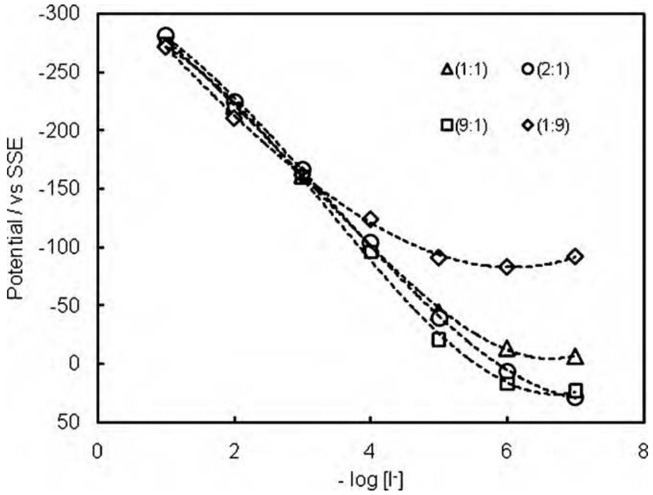

Fig. 3. Potentiometric response of the electrodes with varying concentration of iodide ion.

within <10 s in all the concentration range studied. The same response time was noticed for the reverse process as well. All measurements were made at constant temperature with constant stirring of the solution. The time dependence of electrode response on iodide ion concentration for all 4 electrodes is shown in Fig. 4. The ISE 9:1, ISE 2:1 and ISE 1:1 gave the fast response to iodide ion in the concentration range of 1×10^{-1} to 1×10^{-6} M, while the ISE 1:9 showed the fast response to iodide ion in the concentration range of 1×10^{-1} to 1×10^{-5} M.

Table 2
Response characteristic of various electrodes.

Mole ratio of Ag_2S:AgI	Slope	Linear range
9:1	60.2	1×10^{-1} to 1×10^{-6} M
2:1	54.4	1×10^{-1} to 1×10^{-6} M
1:1	58.7	1×10^{-1} to 1×10^{-6} M
1:9	45.0	1×10^{-1} to 1×10^{-5} M

3.2.4. Electrochemical impedance spectroscopic studies of the electrodes

The interfacial and bulk electrochemical properties of membranes of all the four electrodes were studied using electrochemical impedance spectroscopy (EIS) in the frequency range 20 kHz to 10 mHz at open circuit potential in 10^{-1} M KNO_3, 10^{-3} M KI and 10^{-2} M KI solutions. EIS data were analyzed in terms of equivalent circuit in order to match the measured data. The influence of the electrolyte concentration and composition of membrane material were evaluated.

Fig. 5 shows the model of present electrode with three distinct regions—1st region corresponds to silver back contact/membrane interface, 2nd region corresponds to bulk membrane, and 3rd corresponds to electrolyte membrane interface. In 1st region, there is possibility of electron transfer between silver disk and bulk membrane. In 2nd region, both ionic and electron transfer process are possible as there is Frankel type of lattice defect in bulk membrane where silver ions can migrate from one interstitial site to other interstitial site or in defect sites or push and replace other silver ions while in 3rd region, charge transfer as well as ionic transfer processes are possible.

Fig. 6a–c shows the Nyquist plots of four different electrodes in three different electrolytes 10^{-1} M KNO_3, 10^{-3} M KI, and 10^{-2} M KI, respectively. The points are experimental data. A significant change

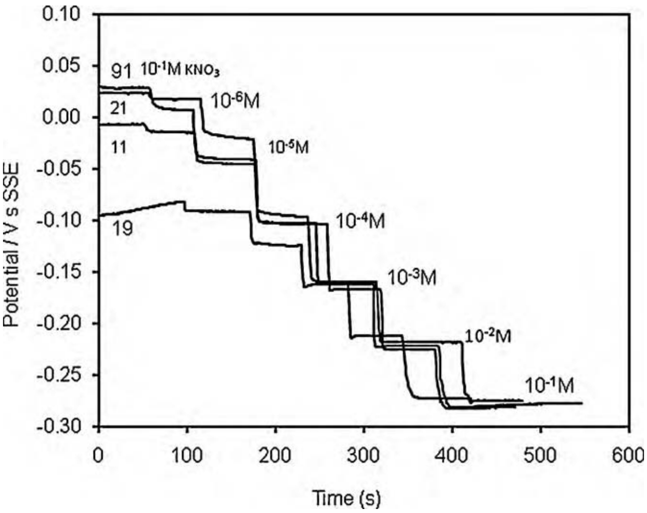

Fig. 4. The dependence of response time of the electrodes on the change of concentration.

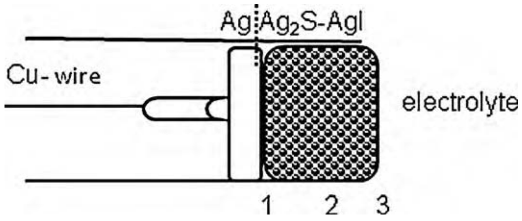

Fig. 5. Electrode model showing three different regions; (1) back contact Ag/Ag_2S, (2) bulk membrane, and (3) membrane–electrolyte interface.

in impedance response can be observed in higher concentration of iodide showing two capacitive loops, one at higher frequency and second one at low frequency.

First capacitive loop is prominent in case of 9:1 electrode whereas it is comparatively small in case of other electrodes. Bralic and Radic have observed a high frequency capacitive loop for back contact in Ag_2S–AgI ISE [22] while Martinhon et al. have observed a distinct semicircle for back contact in case of PbS/Ag_2S ISE [25]. In this study, a distinct capacitive loop for back contact could not be observed due probably to relatively small value of high frequency ac signal.

There are different views regarding the origin of low frequency capacitive loop. Martinhon et al. [25] proposed a diffusion impedance while Bralic et al. [26] has suggested a charge transfer resistance in parallel with a double layer capacitance for low frequency loop. In this study, the low frequency capacitive loop was fitted with both the Warburg diffusion and an RC circuit component. It was found that a good fitting could be only observed by using RC circuit in all the four samples. Therefore, in this study, second capacitive loop was assigned to charge transfer resistance and double layer capacitance at the membrane/electrolyte interface.

Fig. 7 represents the equivalent circuit corresponding to the model of electrode shown in Fig. 5. The lines in Fig. 6a–c show the fitted results by using equivalent circuit in Fig. 7. It is obvious that a good fitting was obtained in all frequency range.

From the fitted data, the membrane/solution resistance and double layer capacitance were obtained, which are given in Table 3. Fig. 8 represents the composition dependence of membrane/solution resistance for different electrodes. The resistance of 1:9 electrode was abnormally high as compared to the resistance of other three electrodes. The enlarged view of Fig. 8, shown in inset, shows that the resistances of ISE 1:1, ISE 2:1, and ISE 9:1 decrease

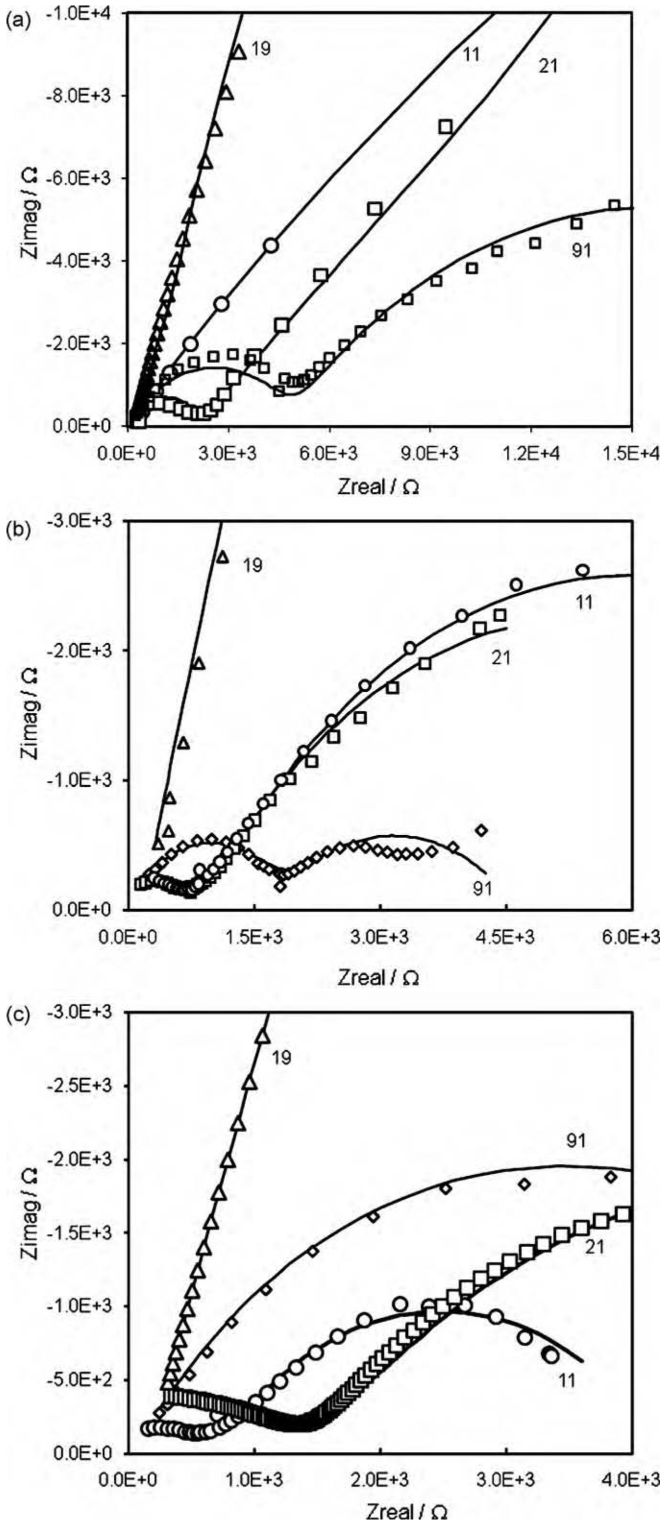

Fig. 6. Nyquist plots of impedance response obtained on various ion selective electrodes in (a) 10^{-1} M KNO_3, (b) 10^{-3} M KI, and (c) 10^{-2} M KI at open circuit potential.

with the increasing mole percentage of Ag_2S [27,28] as Ag_2S is more conductive.

The dependence of double layer capacitance (C_{dl}) with electrode composition is shown in Fig. 9. This plot shows that capacitance of electrode increases with increase in amount of Ag_2S in the electrode.

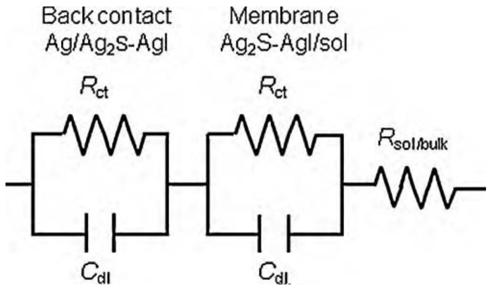

Fig. 7. Equivalent circuit used for fitting the impedance spectra of Fig. 6a–c.

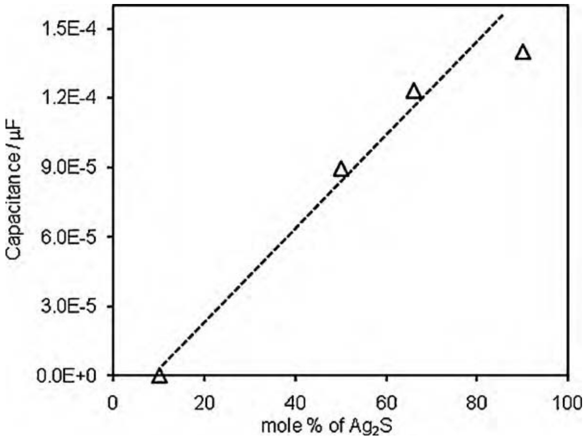

Fig. 8. Variation of the electrode resistance with mole% of silver sulphide. In the inset, enlarged view of low resistance region is shown.

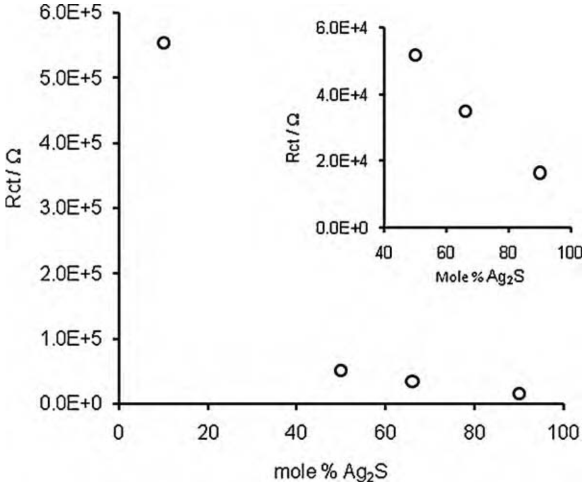

Fig. 9. Variation of electrode capacitance with the mole% of silver sulphide.

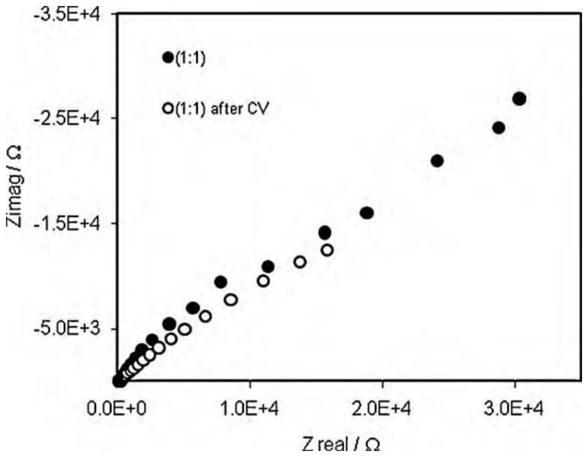

Fig. 10. Nyquist plot of impedance response of ISE 11 before and after CV in 10^{-1} M KNO_3 at open circuit potential.

Fig. 10 shows the impedance spectra recorded before and after performing cyclic voltammetric experiment with ISE 1:1. The impedance of the electrode is observed to decrease after performing the CV showing that electrode become more conductive after running CV. This may be due to the liberation of iodide adsorbed on the surface of the electrode during the CV experiment. It may hence be expected that cyclic voltametric experiment may be used as an alternative way of regenerating electrode surface. This can avoid the loss of membrane material during the polishing of electrode surface.

3.2.5. Visual observation of surface of the electrode

The electrodes were immersed in 0.1 M KI solution for 24 h and surface was observed to see any change. Digital pictures (Fig. 11) show that all four electrode surfaces are affected by high concentration of iodide adsorbed on surface [29]. But the surfaces of ISE 9:1 and ISE 1:9 were found to be more affected than the other two ISEs. Therefore, even though the ISE 9:1 showed good potentiometric response (Fig. 3), its stability is not comparable to that of 1:1 and 2:1 electrodes showing that a significant amount of AgI is essential for stable surface. It has been suggested that during potentiometric measurement AgI may leach out easily from the surface [29] in relatively shorter time. High concentration of AgI on the surface is essential for longer stability of such electrodes. Hence, 1:1 composition of the electrode can be considered as the most suitable composition.

3.2.6. Mott–Schottky analysis of electrode

As ISE 9:1 was found to be not suitable for long-term stability, only three electrodes (1:1, 2:1, and 1:9) were selected for Mott–Schottky analysis to estimate the donor concentration.

When the electrode is polarized with respect to the solution by means of an external emf source, the membrane/electrolyte interface constitutes an electrical double layer with the negative charge is located at the solution side and the corresponding positive charge built up at the semiconductor side. This positive charge will be diffused because of the relatively small charge carrier concentration in the semiconductor. The corresponding sub-surface region in the semiconductor is denoted as the depletion layer. In the case of

Table 3
Fit parameters obtained from the impedance spectra recorded for four different electrodes in 10^{-1} M KNO_3, 10^{-3} M KI, and 10^{-2} M KI solution.

Ag_2S:AgI	10^{-1} M KNO_3		10^{-3} M KI		10^{-3} M KI	
	$R_2/(\Omega)$	$C_2/(\mu F)$	$R_2/(\Omega)$	$C_2/(\mu F)$	$R_2/(\Omega)$	$C_2/(\mu F)$
9:1	1.6×10^4	1.1×10^{-4}	2.9×10^3	2.4×10^{-4}	3.3×10^3	2.7×10^{-5}
2:1	3.5×10^4	1.2×10^{-4}	5.5×10^3	5.6×10^{-4}	3.3×10^3	5.5×10^{-4}
1:1	5.1×10^4	8.9×10^{-5}	9.8×10^3	2.1×10^{-4}	6.8×10^3	3.1×10^{-4}
1:9	5.5×10^5	1.5×10^{-7}	4.5×10^5	1.5×10^{-7}	4.0×10^5	1.5×10^{-7}

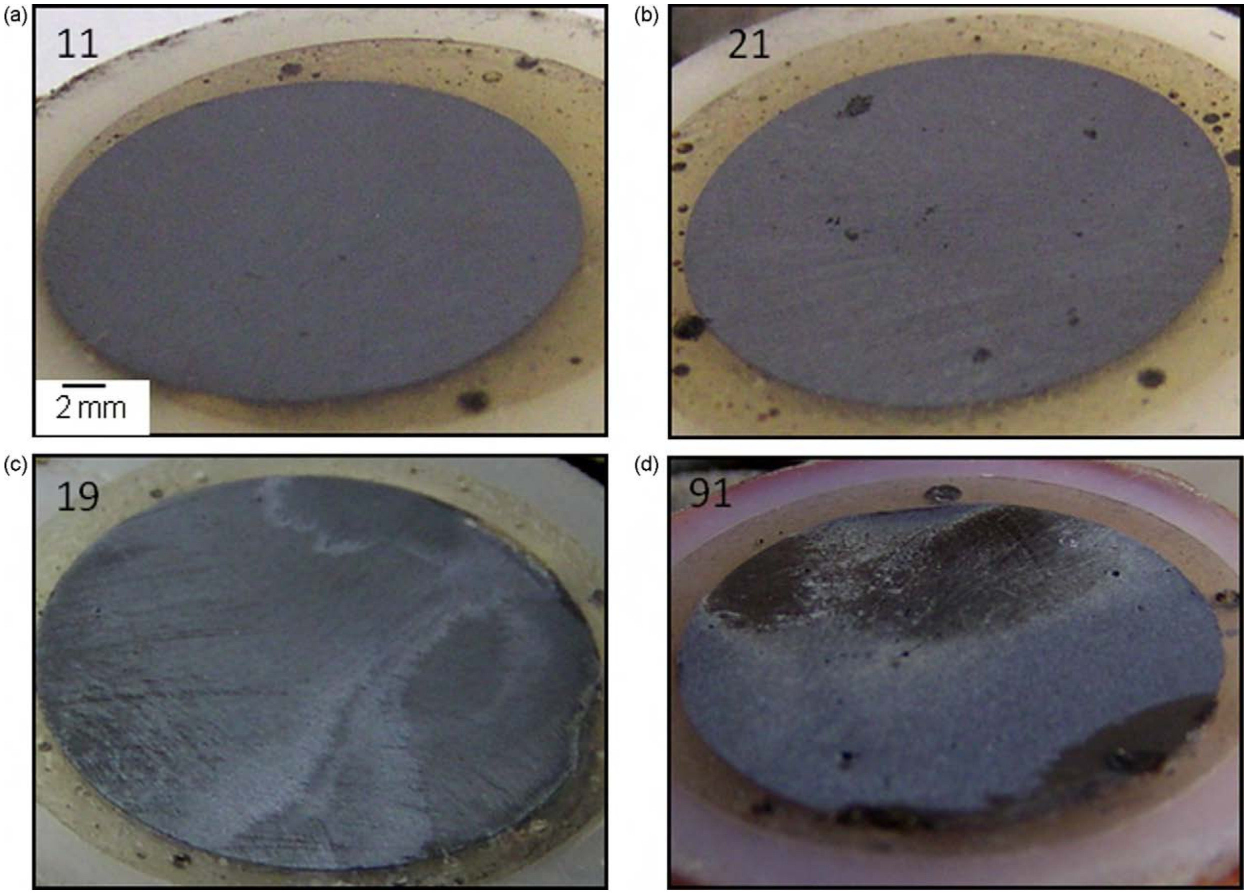

Fig. 11. Digital photos showing the surface of various electrodes after immersion in 10^{-1} M KI for 24 h.

Table 4
Fit parameters obtained from Mott–Schottky analysis.

Mole ratio of Ag_2S:AgI	N_D/(cm^{-3})	E_{fb}/(V)
2:1	2.4×10^{19}	−0.065
1:1	7.4×10^{17}	−0.18
1:9	5.1×10^{14}	−0.05

a depletion of majority electronic carriers near the interface, the interfacial capacitance is developed, which are essentially related to space charge regions in the Ag_2S–AgI electrode and can be used for a Mott–Schottky analysis for the semiconductor properties of electrode. According to the Mott–Schottky Equation (2), the inverse square of C_{sc} should depend linearly on the potential.

$$\frac{1}{{C_{sc}}^2} = \frac{2(E - E_{fb})}{\varepsilon\varepsilon_0 e_0 N_D} \tag{2}$$

where C_{sc} is the space charge layer capacitance, E is the applied potential, E_{fb} is the flat band potential, N_D is the donor density of electrode material, ε_0 is the dielectric permittivity, ε is the relative dielectric constant, e_0 is the elementary charge.

A Mott–Schottky plot of $1/C_{sc}^2$ against applied potential (E) is presented in Fig. 12. A straight line with positive slope $2/e\,\varepsilon\varepsilon_0\,N_D$ is observed between +0.2 V and −0.2 V (SSE) indicating n-type semiconductor behaviors of polycrystalline Ag_2S–AgI membrane. The donor concentration N_D was calculated from the slope using dielectric constant of Ag_2S–AgI. The flat band potential was determined by extrapolation of the linear region of the Mott–Schottky plot. The donor defect concentration and flat band potential obtained by Mott–Schottky analysis are tabulated in Table 4.

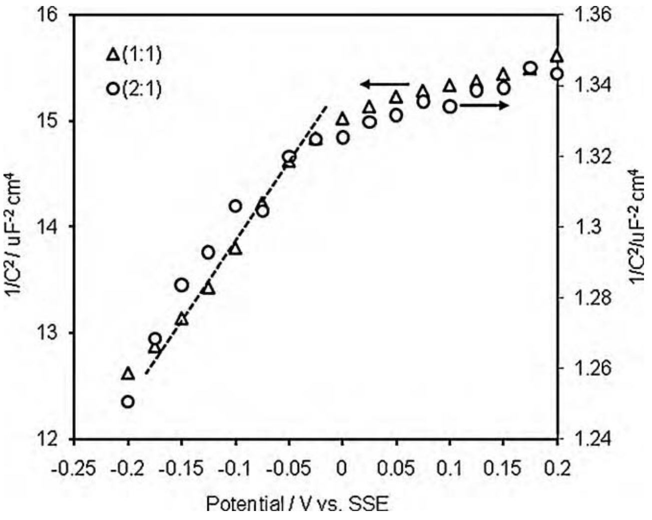

Fig. 12. Mott–Schottky plot of 1:1 and 2:1 electrodes in 10^{-1} M KNO_3.

The donor defect concentration (N_D) of 1:9 electrodes is lower than 1:1 and 2:1 electrodes. When 1:9 electrodes are used for long periods of time, surface got deteriorated as shown in Fig. 11. Hence, the N_D values of 1:9 electrode is comparably lower than 1:1 and 2:1 electrodes. The values obtained were about six orders of magnitude lower than in metals. This is an important implication for the charge and potential distribution at the semiconductor/electrolyte interface [30]. The sub-Nernstian response of 1:9 electrodes is due to low N_D value compared to others.

4. Conclusion

Based on the above results the following conclusions can be made:

1. X-ray diffraction studies show that the laboratory prepared Ag_2S–AgI co-precipitates are composed of Ag_3SI, Ag_2S and AgI components showing mixed phase state of the material.
2. The electrode surface became smoother and lustrous with the increasing concentration of Ag_2S in AgI.
3. The home-made Ag_2S/AgI electrodes having three different compositions (1:1, 2:1, 9:1) show a Nernstian response over a wide concentration range of iodide ions (10^{-1} to 10^{-6} M) while the electrode having 1:9 composition shows sub-Nernstian behavior up to the concentration range of (10^{-1} to 10^{-5} M).
4. All the four electrodes have quick response time (<10 s).
5. The EIS results clearly showed that mixing of silver sulphide with silver iodide decreases the membrane resistance and increases the capacitance by a few orders of magnitude. About 50 percentage of iodide in membrane is preferable to increase the sensitivity and stability of the electrode.
6. Mott–Schottky analysis of electrodes in aqueous electrolytes shows n-type semiconductor behavior with a donor density of a reasonable order of magnitude for a polycrystalline material.
7. The visual observation showed that in comparison to others, the 1:1 electrode is less affected by iodide ions while storing in iodide solution.

Acknowledgements

A. Rajbhandari (Nyachhyon) thanks Tribhuvan University for granting study leave and to the Nepal Academy of Science and Technology (NAST) for providing PhD scholarship to carry out this work. The authors gratefully acknowledge Tsuru–Nishikata laboratory, Tokyo Institute of Technology, Tokyo, for providing facilities to record SEM, EIS and CV of the material.

References

[1] E. Pungor, K. Toth, P.G. Klatsmanyi, K. Izutsu, Pure Appl. Chem. 55 (1983) 2029.
[2] I.M.S. Lopes Teresa, O.S.S. Rangel Antonio, J.L.F.C. Lima, M. Conceicao, Anal. Chim. Acta 308 (1995) 122.
[3] R. Perez Almos, A. Rios, J.R. Fernandez, R.A.S. Lapa, J.L.F.C. Lima, Talanta 53 (2001) 741.
[4] J.L.F.C. Lima, M. Conceicao, B.S.M. Montenegro, L.M. Ivanildo, G.O. Neto, J.A. Gomes, E.A.G. Zagatto, Talanta 40 (1993) 1563.
[5] J. Barbosa, D. Barron, S. Butti, I. Marques, Polyhedron 18 (1999) 3361.
[6] P.L. Bailey, Analysis with Ion Selective Electrodes, Heyden and Son, London, 1980.
[7] J.F. Lechner, I. Sekerka, J. Electroanal. Chem. 57 (1974) 317.
[8] I. Sekerka, F. Lechner, J. Electroanal. Chem. 69 (1976) 339.
[9] J. Bagg, G.A. Rechniz, Anal. Chem. 45 (1973) 271.
[10] M.H. Sorrentino, G.A. Rechniz, Anal. Chem. 46 (1974) 943.
[11] M. Mascini, A. Liberti, Anal. Chim. Acta 64 (1973) 64.
[12] M.J.D. Brand, J.J. Militello, G.A. Rechniz, Anal. Lett. 2 (1969) 523.
[13] M. Mascini, A. Liberti, Anal. Chim. Acta 60 (1972) 405.
[14] Orion Research Inc., Newsletter 2 (1970) 41.
[15] E. Pungor, J. Havas, K. Toth, Acta Chim. Acad. Sci. Hung. 41 (1964) 239.
[16] E. Pungor, J. Havas, K. Toth, Anal. Chem. 5 (1965) 9.
[17] J. Ruziicka, C.G. Lamm, Anal. Chim. Acta 54 (1971) 1–12.
[18] A. Rajbhandari (Nyachhyon), A.P. Yadav, K. Manandhar, R.R. Pradhananga, Scientific World, vol. 7, 2009, p. 19.
[19] R.P. Buck, D.E. Mathis, R.K. Rhodes, J. Electroanal. chem. 60 (1971) 245.
[20] R.K. Rhodes, R.P. Buck, J. Electroanal. chem. 86 (1978) 349.
[21] R.P. Buck, Ion Selective Electrode Rev. 4 (1982) 3.
[22] M. Bralic, N. Radic, Chroatica Chem. Acta 67 (1994) 543.
[23] A.J. Bard, L.R. Faulker, Electrochemical Methods—Fundamentals and Applications, Wiley, New York, 1980.
[24] G.H. Jaffery, J. Bassett, J. Mendham, R.C. Denny, Textbook of Quantitative Analysis, 5th ed., 1996.
[25] P.T. Martinhon, J. Carrenno, C.R. Sousa, O.E. Barcia, O.R. Mattos, Electrochim. Acta 51 (2006) 3022–3028.
[26] M. Bralic, N. Radic, S. Brinic, E. Generalic, Talanta 55 (2001) 581–586.
[27] M. Gratzl, E. Pungor, Anal. Chim. Acta 1 (89) (1986) 217–228.
[28] R.P. Buck, Anal. Chem. 46 (1973) 28R.
[29] E.G. Harsannyi, K. Toth, L. Polos, E. Pungor, Anal. Chem. 54 (1982) 1094–1097.
[30] W.P. Gomes, D. Vanmaekelbergh, Electrochim. Acta 41 (1996) 967–973.